ISIJ International, Vol. 59 (2019), No. 2, pp. 293–299

Generation Mechanism of Driving Out Force of the Shaft from the Shrink Fitted Ceramic Roll by Introducing Newly Designed Stopper

Guowei ZHANG, Hiromasa SAKAI, Nao-Aki NODA,* Yoshikazu SANO and Shun OSHIRO

Dept. of Mechanical and Control Engineering, Kyushu Institute of Technology, 1-1 Sensui-cho, Tobata-ku, Kitakyushu-shi, 804-8550 Japan.

(*Received on September 4, 2018; accepted on October 11, 2018; originally published in Tetsu-to-Hagané, Vol. 104, 2018, No. 11, pp. 620–627*)

Ceramic roller can be used in the heating furnace conveniently because of its high temperature resistance. The roller consists of ceramic sleeve and steel shaft connected only under a small shrink fitting ratio because of the brittleness. However, the coming out of the shaft sometimes happens from the ceramic sleeve under repeated loading. Therefore, it is important to find out the driving out force to prevent the coming out failure. Based on the previous studies, a two-dimensional shrink fitted structure is considered by replacing the shaft with the inner plate and by replacing the sleeve with the outer plate. Then, the driving out force is focused in this study by introducing a newly designed stopper on the outer plate. The finite element simulation shows that the coming out phenomenon can be prevented due to the stopper installed on the outer plate. Then the mechanism of driving out force generation is clarified. Finally, the process of coming out is explained in terms of the residual displacement.

KEY WORDS: shrink fitting; ceramic roller; driving out; stopper; residual displacement.

1. Introduction

Steel conveying rollers are used in the heating furnace as shown in **Fig. 1** for producing high-quality steel plates. The conventional common roller uses the steel material with ceramic spray coating on outside of the sleeve. Inside of the roller is cooled by water for reducing the temperature. Since the linear expansion coefficient of steel is about 4 times larger than that of ceramics, the thermal expansion mismatch may exceed the strength of the ceramic layer and may cause failure on the roller surface such as wearing, peeling and crack.[1] Therefore, it is difficult to maintain a long life for such rollers.

Figure 2 illustrates a new ceramic roller consisting of the steel shaft connected at both ends and the ceramic sleeve having high heat resistance, high wear resistance and high corrosion resistance.[2,3] Previous studies indicated that the shrink fitting system may be the most suitable joining method for ceramic cylindrical structures to reduce maintenance time and cost for shaft replacement.[4–8] However, since most of the ceramics are quite brittle, only a small shrink fitting ratio can be used.[9–16] During operation, the coming out of the shaft may happen, and therefore, we have to prepare for this new failure.

In our previous studies, coming out simulations were performed for the shaft from the shrink-fitted ceramic sleeve by using the finite element method.[4,5] In Ref.,[4] a three-dimensional roller model was considered by replacing the roller rotation as the load shifting on the fixed roller. Since the calculation time was very large, only the rotation cycles until $N = 5$ were conducted. Then, effects of shrink fitting ratio, friction coefficient *et al.* on the coming out behavior were studied. Furthermore, in Ref.,[5] the two-dimensional simulation was conducted to reduce the calculation time and more than $N = 40$ cycles were investigated. Those studies[4,5] have proved that the coming out behavior can be numerically realized on the two-dimensional and three-dimensional simulations.

As a further development of those previous studies, this study will focus on a stopper newly installed on the sleeve

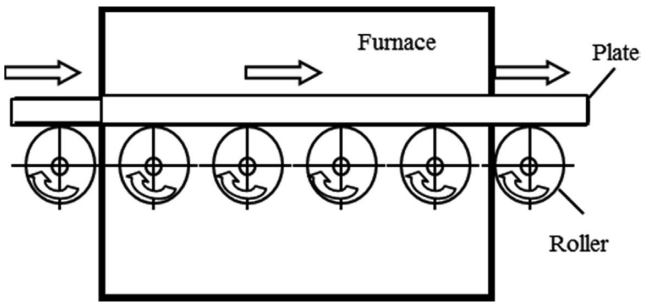

Fig. 1. Layout of rollers in heating furnace.

* Corresponding author: E-mail: noda.naoaki844@mail.kyutech.ac.jp
DOI: https://doi.org/10.2355/isijinternational.ISIJINT-2018-615

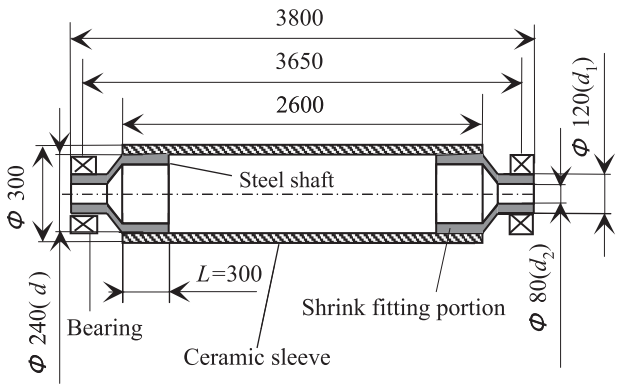

Fig. 2. Structure and dimensions of a real ceramic roller (Unit:mm).

to evaluate the driving out force generated on the shaft. In the first place, a two-dimensional model used in Ref.[5] will be improved to prevent the coming out. To design the stopper, the contact force will be investigated between the stopper and the inner plate. Note that this contact force can be regarded as the driving out force generated on the shaft. The discussion shown in this paper is therefore useful for understanding the coming out mechanism as well as the practical aspect of the coming out prevention.

2. Analysis Method

In this research, in the first place, the coming out behavior will be simulated by using the elastic finite element method analysis. Next, after confirming the contact between the inner plate and the stopper, the driving out force of the coming out will be studied from the contact force.

The two-dimensional analytical model used in the previous paper[5] is shown in **Fig. 3**. To simulate the behavior in a large number of cycles, the shaft is replaced by the inner plate and the sleeve is modeled as the outer plate as shown in Fig. 3. The coming out behavior is analyzed by paying attention to the displacement at Point C.

Figure 4(a) illustrates the new 2D model having the stopper whose height = 1.6 mm. The detail of the stopper part is shown in Fig. 4(b). Consider Point D in Fig. 4(b) as the reference point for the coming out displacement of the inner plate. To simplify the analysis, the outer plate is assumed as a rigid body. The inner plate combines the steel and filler together by considering equivalent elastic modulus. This is because the hollow structure cannot be used in the 2D simulation.[5,17] **Table 1** shows the material properties of the model. The outer plate and the inner plate are connected by shrink fitting. The shrink fitting ratio is defined as the shrink fitting value δ divided by the thickness d of the outer plate fitting portion (d = 240 mm). The shrink fitting ratio δ/d ranges from 0 to 1.0×10^{-3}. Here, in order to elucidate the basic generation mechanism of the driving out force, the shrink fitting ratio δ/d = 0.2×10^{-3}, the friction coefficient μ = 0.3, the stopper height H = 1.6 mm are used as reference values. The boundary conditions are the same as described in the previous paper.[5]

In this study, since the inertial force can be neglected,[4] a quasi-static elastic structure analysis is performed by using MSC Marc/Mentat 2012 with full Newton-Rapson

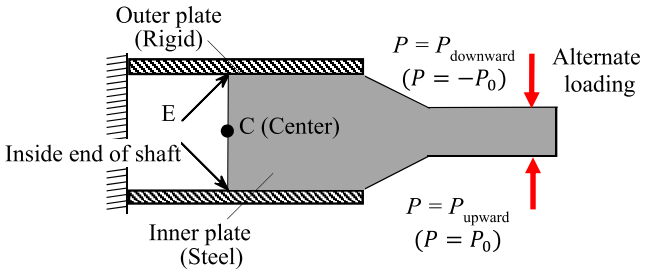

Fig. 3. 2D model considered in the previous paper.[5] (Online version in color.)

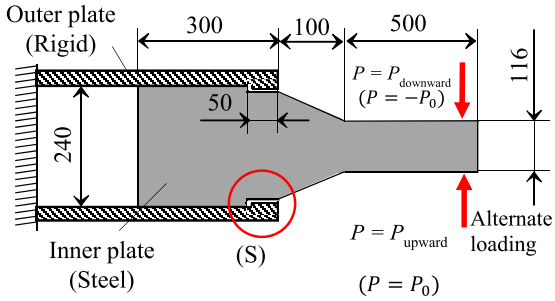

(a) 2D model with stopper (mm)

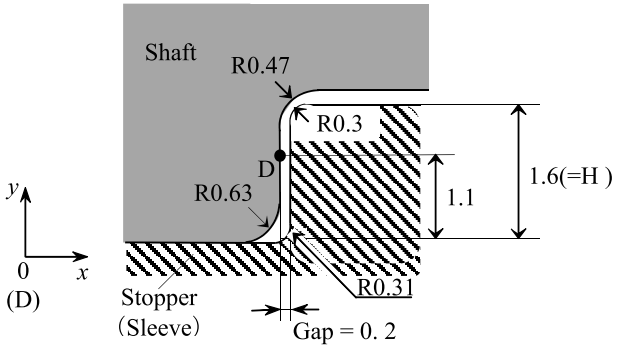

(b) Detail of stopper (S) (mm)

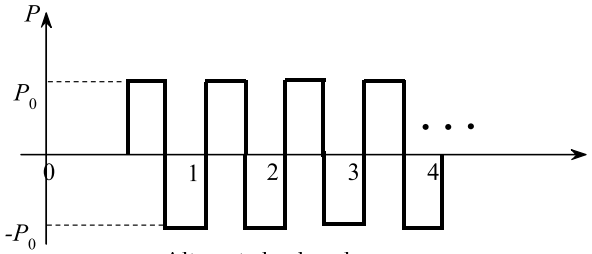

Alternate load cycles

(c) Alternate loading

Fig. 4. New simplified 2D model with stopper. (Online version in color.)

Table 1. Material properties.

Model	2D		
	Sleeve	Shaft	
	Rigid	Steel	Filler
Young's modulus [GPa]	∞	210	52
Poisson's ratio	–	0.3	0.3
Tensile strength [MPa]	∞	600	–
Mass density [kg/m^3]	0	7 800	7 800

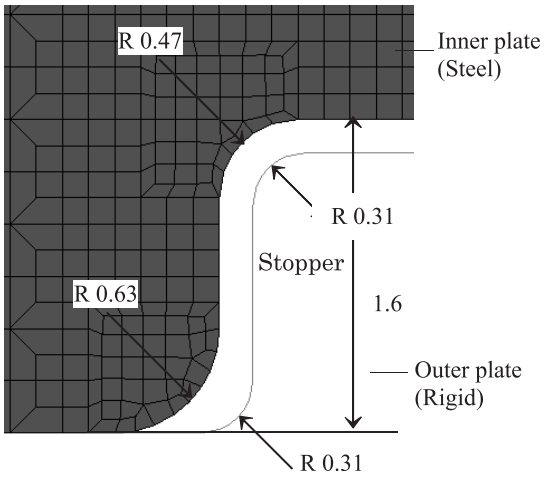

Fig. 5. Mesh detail of the inner plate around stopper (see Fig. 4(b)) (Unit:mm).

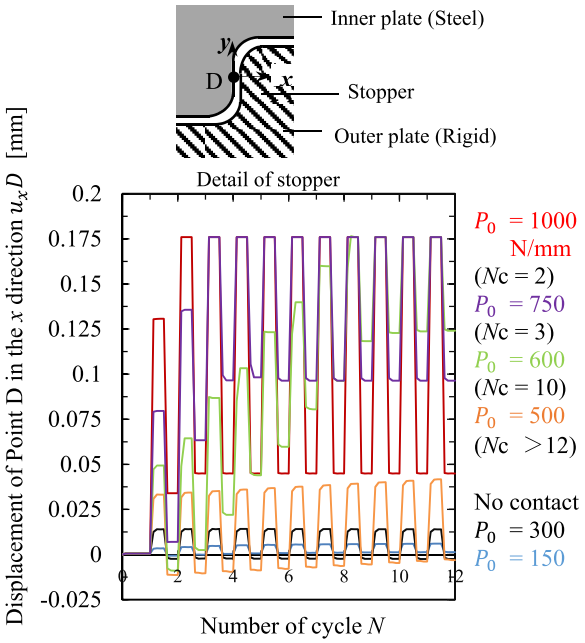

Fig. 6. Displacement u_{xD} vs number of cycle N under different loads, fixed shrink fitting ratio $\delta/d = 0.2\times10^{-3}$ and friction coefficient $\mu = 0.3$. (Online version in color.)

iterative sparse solver of multifrontal method.[18] Considering the symmetry of the model, alternate loads are applied in the vertical direction to the 1/2 model as shown in Fig. 4(a). Here, the quadrangular contact element has been used and the number of element is 24546. In contact analysis by MSC Marc/Mentat 2012, it has been told that the Coulomb friction model can be widely used for most practical applications except for bulk forming as encountered in *e.g.* forging processes. Three types of Coulomb friction models are avilable,[19] that is, arctangent model, stick-slip model and bilinear model. However, it is known that the arctangent model is unsuitable for estimating the typical relative sliding velocity priori when the sliding velocity varies largely during the analysis. Also, the stick-slip model needs a large amount of data to be determined from repetitive calculation process.[19] In this study, therefore, the bilinear model is applied since the friction force is simply determined from the displacement. **Figure 5** shows the mesh detail around the stopper and the minimum element size is 0.15625×0.15625 mm.

3. Conditions and Mechanism for the Driving Out Force Generation

3.1. Generation Conditions of the Driving Out Force

When alternate load P is repeatedly applied to the inner plate in N cycles, a kind of driving out force may be generated on the inner plate. Then, the inner plate comes out gradually. However, in this study, since the stopper is installed on the outer plate, the movement of the inner plate in the axial direction can be stopped by the stopper. Here, Point D at 1.1 mm distance from the fitting surface is used to represent the contact point, the number N_c denotes the cycle when the contacting starts. To describe the contact condition at the stopper, the coming out of the inner plate is represented by the displacement u_{xD} in the x-direction.

Figure 6 shows displacement u_{xD} in different loading cycles under alternate loading P. Here, the reference values, $\delta/d = 0.2\times10^{-3}$ and μ=0.3 are used. In Fig. 6, before loading $N < 1$, a small displacement $u_{xD} = 0.000537$ mm caused by shrink fitting is ignored and $u_{xD} = 0$ mm is assumed before shrink fitting. When the load becomes large, the displacement u_{xD} increases with increasing N, then becomes stable after the inner plate contacts with the stopper. For example, when P = 1 000 N/mm, the displacement reaches a constant value of 0.176 mm during the second cycle and does not change anymore. This is because u_{xD} = 0.176 mm means that the point D contacts with the stopper. With decreasing P, the contact starting cycle N_c increases, and when P is small enough, no contact occurs. Therefore, there is a threshold value P for the coming out. From Fig. 6, the threshold value of P is between 150 N/mm and 300 N/mm. When the load P is below this threshold, the displacement u_{xD} does not increase and the inner plate does not contact with the stopper. When the load P is above the threshold, the displacement u_{xD} increases with increasing cycles N. In Fig. 6, the driving out force appears if P > 300 N/mm for the reference condition $\delta/d = 0.2\times10^{-3}$ and μ = 0.3.

Note that the contact occurs at u_{xD} = 0.176 mm smaller than the gap amount 0.2 mm. The reason can be explained in the following way. To handle the contact problem, the amount of the contact judgement should be larger than the single side fitting amount $\delta/2$ for Msc.Marc/Mentat 2012.[19] In this study, since $\delta/d = 0.2\times10^{-3}$ and d = 240 mm, we have $\delta = 0.2\times10^{-3} \times 240 = 0.048$ mm. Therefore, the single side fitting amount $\delta/2 = 0.048\times1/2 = 0.024$ mm. Since u_{xD} = 0.176 mm is 0.024 mm smaller than the gap 0.2 mm, in Fig. 6, the displacement u_{xD} = 0.176 mm should be regarded as the contact distance between the inner plate and the stopper.[20]

3.2. Generation Mechanism of the Driving Out Force

In this simulation, the inner plate is prevented from coming out by the stopper. Then the contact force F_s can be regarded as the driving out force. **Figure 7** shows the relationship between the load P and the contact force F_s by changing the friction coefficient μ. Here, the cycle N = 100 is the maximum cycle number. When the largest friction coefficient μ = 0.5, it can be seen that there is no coming

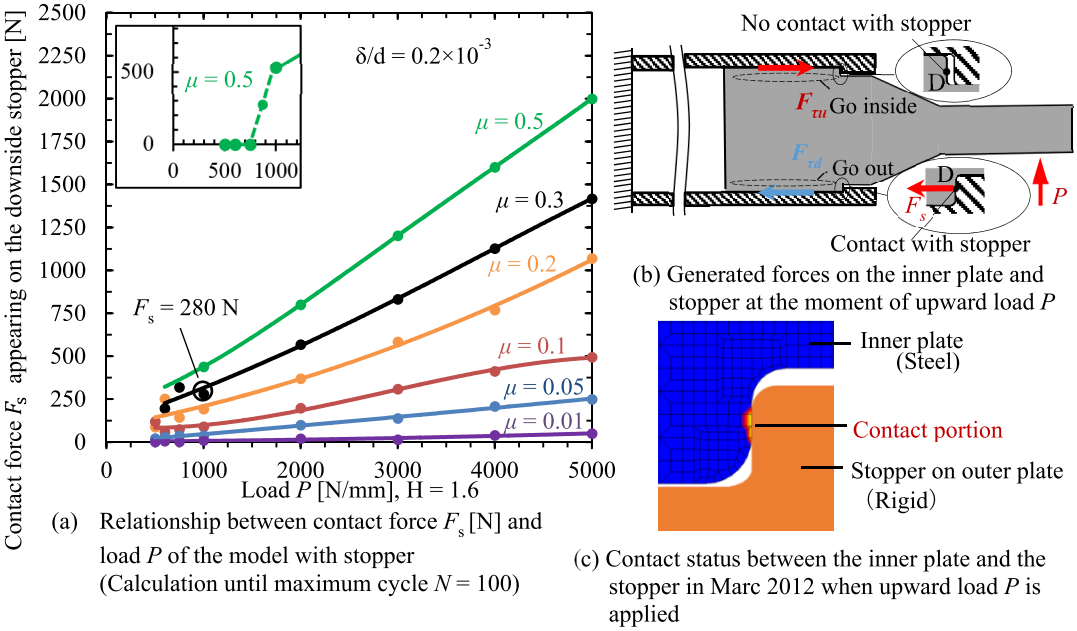

(a) Relationship between contact force F_s [N] and load P of the model with stopper (Calculation until maximum cycle N = 100)

(b) Generated forces on the inner plate and stopper at the moment of upward load P

(c) Contact status between the inner plate and the stopper in Marc 2012 when upward load P is applied

Fig. 7. Relationship between load P and contact force F_s under different friction coefficient μ when the upward load P is applied and $\delta/d = 0.2\times10^{-3}$. (Online version in color.)

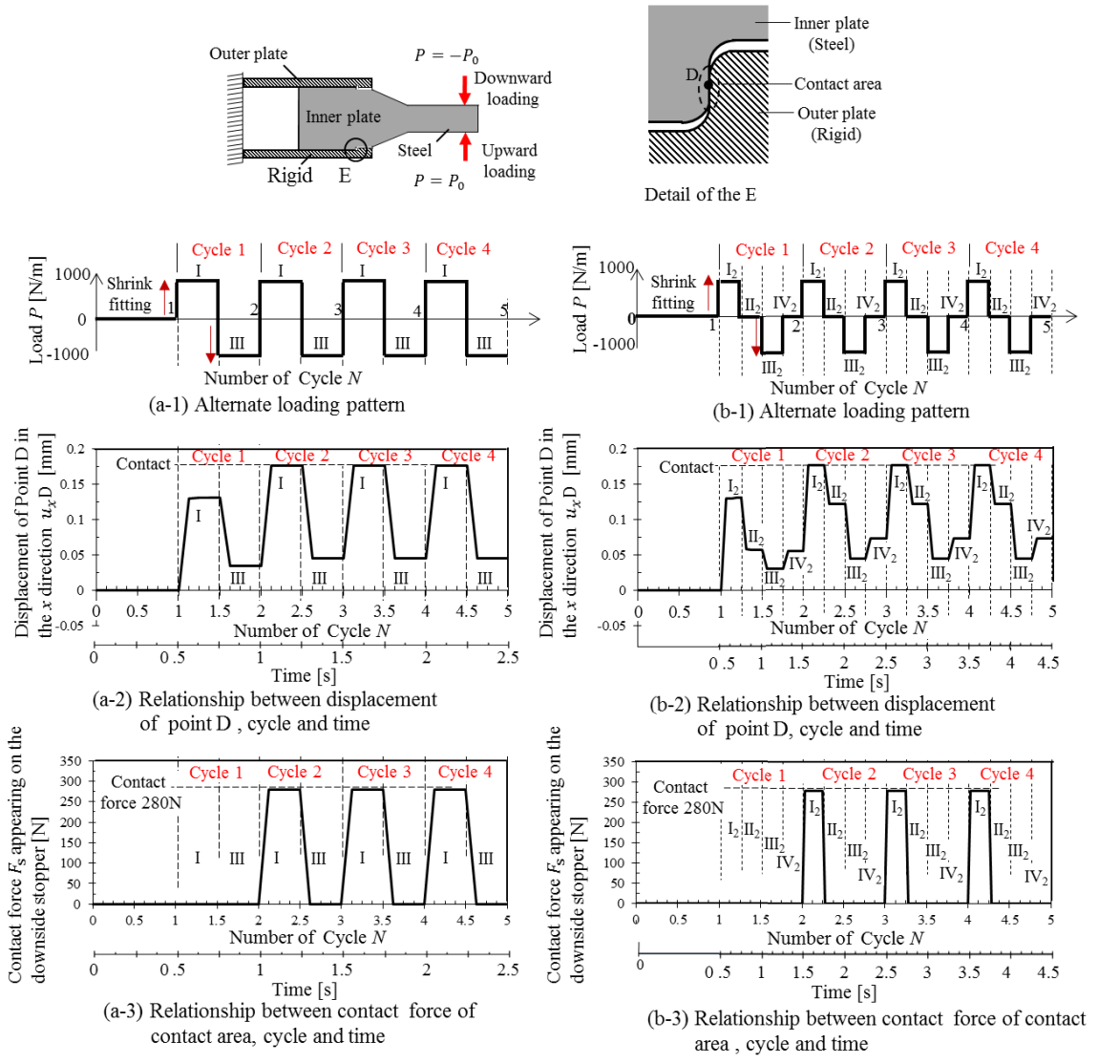

(a-1) Alternate loading pattern

(b-1) Alternate loading pattern

(a-2) Relationship between displacement of point D , cycle and time

(b-2) Relationship between displacement of point D, cycle and time

(a-3) Relationship between contact force of contact area, cycle and time

(b-3) Relationship between contact force of contact area , cycle and time

(a) Load (a-1) causes displacement (a-2) and contact force F_s(a-3)

(b) Load (b-1) causes displacement (b-2) and contact force F_s(b-3)

Fig. 8. Displacement of Point D and contact force F_s when load P = 1 000 N/mm, μ = 0.3, $\delta/d = 0.2\times10^{-3}$. (Online version in color.)

out when $P \leq 750$ N/mm. As shown in Fig. 7(a), when $P \geq 875$ N/mm the contact force F_s increases with increasing load P. When $\mu = 0.3$, F_s increases almost proportionally with increasing load P when $P \geq 600$ N/mm.

In Fig. 7, with decreasing the friction coefficient μ, the contact force F_s decreases. When there is no friction as $\mu = 0$, F_s does not appear. In this way, it is seen that the contact force F_s is controlled by the friction coefficient μ of the fitting surface.

When the inner plate is subjected to the alternate loading P, the frictional shearing force generated on the fitting surface is balanced with the contact force F_s at the stopper. In Fig. 7(b), from the shearing force $F_{\tau u}$ on the upside surface and the shearing force $F_{\tau d}$ on the downside surface, the contact force F_s can be expressed as the following equation.

$$F_s = F_{\tau u} + F_{\tau d} \quad \text{..... (1)}$$

For example, in Fig. 7(a), under $P = 1\,000$ N/mm and $\mu = 0.3$, when the inner plate contacts with the stopper, we have $F_{\tau u} = 1\,272$ N, $F_{\tau d} = -992$ N. By substituting into Eq. (1) we have a contact force $F_s = 280$ N, which can be regarded as the driving out force.

4. Discussion on the Coming Out Process

4.1. Relationship between the Displacement of the Inner Plate and the Contact Force

In the previous section, the effect of the magnitude P and

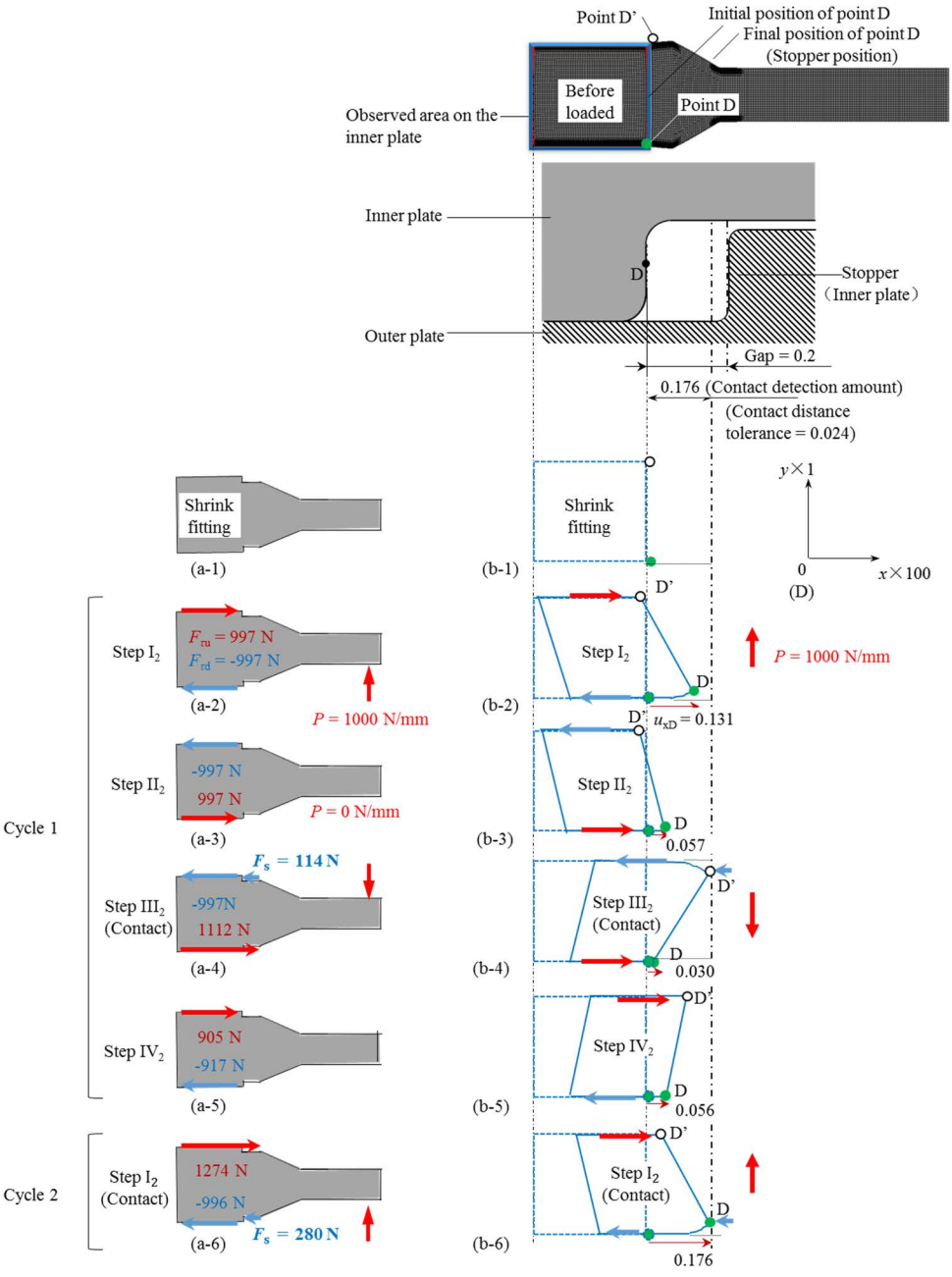

(a) Shear force and balance of the inner plate

(b) Coming out process of the inner plate including displacement u_{xD} and deformation

Fig. 9. The coming out process of the inner plate when the load is 1 000 N/mm in the 1st, 2nd cycle (mm). (Online version in color.)

the friction coefficient μ on the coming out has been considered by focusing on the displacement u_{xD} at Point D. This section considers how the displacement u_{xD} and the contact force F_s appear and increase under the alternate loading.

Figure 8 shows the displacement at Point D and the contact force appearing at the downside stopper under the loads in Figs. 8(a-1) and 8(b-1). Here, the reference values P = 1 000 N/mm, μ = 0.3, δ/d = 0.2 × 10^{-3} are used in the simulation. Under the loading in Fig. 8(a-1), the displacement is shown in Fig. 8(a-2) and the contact force is shown in Fig. 8(a-3). In contrast to Fig. 8(a-1), as shown in Fig. 8(b-1), the no-load interval is newly added between alternate loading. This is to clarify the coming out process by considering the displacement under no loading period. Fig. 8(a-2) shows the displacement u_{xD} corresponding to the load pattern of Fig. 8(a-1). The upward load (step I) and the subsequent downward load (step III) compose the first cycle. Figure 8(b) shows that the load (b-1) causes the displacement (b-2) different from the one in Fig. 8(a-2). As shown in Fig. 8(b-2), in the second cycle where the contact force becomes stable, it is seen that the displacement of step II_2 under the downward load is larger than the step IV_2 under the upward load. New displacement steps II_2, IV_2 appear during the no-load interval. Depending on the direction of the applied load, different displacements occur irreversibly even under the no-load step. This irreversible behavior may cause the coming out behavior. The remaining displacement under no-load step is called 'residual displacement' in this study.

4.2. Coming Out Process Explained in Terms of the Residual Displacement

This section focuses on the entire fitting area of the inner plate including point D. Then, the residual displacement will be considered to explain the coming out. **Figure 9** shows the coming out process under the loading in Fig. 8(b-1). Figure 9(a) shows the equilibrium between the frictional shearing force generated and the contact force at the stopper. Figure 9(b) shows the deformation and the displacement over the entire fitting portion. The dotted line shows the entire fitting portion shape after shrink fitting and before alternate loading. The solid line shows the deformation and the displacement under loading. In Fig. 9(b), the deformation is enlarged in the x-direction for the reader's convenience.

When the first upward load (step I_2 in Figs. 8(b-2) and 9(b-2)) is applied, Point D moves in the coming out direction, but does not contact with the stopper. Then, the shear forces on the upside and downside surfaces of the inner plate are balanced. In the no-load interval (step II_2), Point D goes back to the inward direction but does not return completely. Therefore, Point D is in the residual displacement state. Here, the shearing forces change the directions but still maintain the balance. Next, in step III_2 where a downward load is applied, Point D' on the upper surface comes into contact with the stopper while slight displacement of Point D in the coming out direction has been left. The contact force of upside stopper is 114 N which does not reach the full contact force 280 N appearing at the second cycle of step I_2. In this step III_2, the residual displacements are generated in both of the upside and downside, and therefore, the coming out process has been analytically demonstrated.

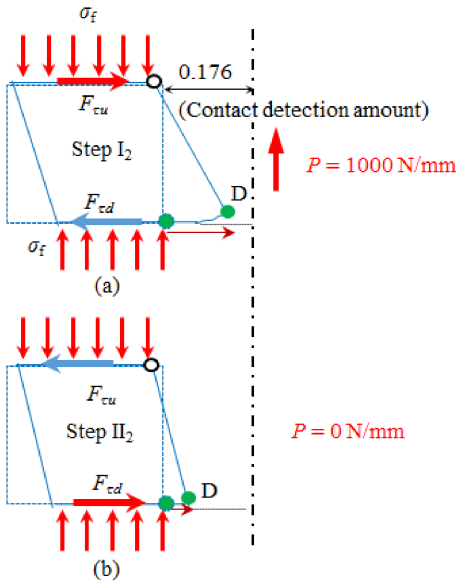

Fig. 10. Schematic diagram of the mechanism of residual displacement of the inner plate (mm). (Online version in color.)

At the end of the first cycle (step IV_2, no load), both of the residual displacements of Point D and Point D' keep on moving in the coming out direction, and the coming out behavior of the entire inner plate becomes significant. Although the residual displacement of Point D at the end of the second cycle increases, it becomes stable in the subsequent cycle as shown in Fig. 8(b-2). Next, the reason why the residual displacement occurs will be explained during the coming out simulation.

Figure 10 compares the deformation and the displacement over the entire fitting portion (a) under the upward loading and (b) after removing the upward loading. Here, the fitting pressure σ_f always exists along the fitting portion. When the upward load is applied, shearing forces $F_{\tau u}$, $F_{\tau d}$ occur along the fitting surface so as to maintain the balance with the moment caused by the loading. Therefore, the fitting portion is deformed into a diamond shape, Point D moves in the coming out direction, and Point D' moves in the opposite direction. When the bending load P is removed, since the moment due to the external force disappears, the diamond shape of the fitting portion tries to return to the original shape. Then, the deformation around Point D decreases, but the deformation is restricted by the reverse shearing force caused by the fitting pressure and friction. Therefore, Point D does not return to the original shape completely and the residual displacement remains. Accumulation of this residual displacement causes the inner plate coming out. It can be seen that the presence of fitting pressure and the friction dominate the deformation, which results in the residual displacement. In this way, the shaft coming out process can be explained in terms of the residual displacement.

4.3. Application to the Shrink-fitting Roller

In previous studies,[4] without stopper (see Fig. 2), the three-dimensional coming out simulation was carried out by replacing the rotation under bending load as the load shift on the fixed roller. Subsequently, a two-dimensional simula-

tion was conducted under an alternate loading.[5] Then, the coming out phenomenon was realized by using the two-dimensional simulation, which can be applied to the three-dimensional shape. In this study, a new model with stoppers was considered in two-dimensional simulation similarly to the previous studies. The coming out process has been clarified in this study, and this approach can also be applied to the three-dimensional roller to prevent coming out.

5. Conclusions

In this paper, by developing our previous studies, the driving out force was discussed to design the ceramic rolls. To simplify the three-dimensional roller, two-dimensional simulation was considered by adding the stopper to prevent coming out. The contact force at the stopper is regarded as the driving out force. To explain the driving out force generation mechanism, the equilibrated forces were considered among the frictional shear forces and the contact force. The coming out process was also explained in terms of the residual displacement. The conclusions can be summarized in the following way.

(1) Shear forces are generated along the upside and downside at the fitting portions of the inner plate to balance the alternate bending load. The inner plate comes out gradually when the shear forces in the coming out direction exceeds the shear force in the opposite direction.

(2) When the alternate loading is applied under the condition of (1), the inner plate and the stopper come into contact with each other. The contact force generated on the stopper can be regarded as the driving out force.

(3) In order to clarify the coming out phenomenon and generation mechanism, no-load interval was introduced into the alternate bending loading cycle. As a result, it was found that the residual displacement appears during the no-loading interval. The coming out process can be explained by the accumulation of this residual displacement.

(4) The driving out force can be generated by the shrink fitting force, the friction force, and the bending load as shown in Fig. 10.

Acknowledgement

The authors wish to express our thanks to the members of our group, Dedi SURYADI, Yuanming XU, Yuuki YASUI for their kind support for this study.

REFERENCES

1) M. Fujii, A. Yoshida, J. Ishimaru, S. Shigemura and K. Tani: *Trans. Jpn. Soc. Mech. Eng. C*, **72** (2006), 1354 (in Japanese).
2) C. R. Liou, T. Mori, H. Kobayashi and T. Mitamura: *JCS-Jpn.*, **98** (1990), 348 (in Japanese).
3) T. Ono: *J. Jpn. Soc. Mech. Eng.*, **86** (1983), 470.
4) N.-A. Noda, D. Suryadi, S. Kumasaki, Y. Sano and Y. Takase: *Eng. Fail. Anal.*, **57** (2015), 219.
5) N.-A. Noda, Y. Xu, Y. Sano and Y. Takase: *ISIJ Int.*, **56** (2016), 303.
6) W. Li, N.-A. Noda, H. Sakai and Y. Takase: *J. Solid Mech. Mater. Eng.*, **5** (2011), 14.
7) W. Li, N.-A. Noda, H. Sakai and Y. Takase: *Key Eng. Mater.*, **452** (2011), 241.
8) A. Rusin, G. Nowak and W. Piecha: *Eng. Fail. Anal.*, **34** (2013), 217.
9) E. Ogawa, K. Shimizu, S. Hamayoshi, N. Kumagai, Y. Ohtsubo, N.-A. Noda, Y. Takase, K. Kishi, K. Shobu, T. Tabaru, E. Maeda, S. Koga and T. Matsuda: *Hitachi Met. Tech. Rev.*, **28** (2012), 50 (in Japanese).
10) M. Tsuyunaru, N.-A. Noda, Hendra and Y. Takase: *Trans. Jpn. Soc. Mech. Eng. A*, **74** (2008), 919 (in Japanese).
11) N.-A. Noda, Hendra, Y. Takase and M. Tsuyunaru: *J. Solid Mech. Mater. Eng.*, **2** (2008), 1410.
12) N.-A. Noda, M. Yamada, Y. Sano, S. Sugiyama and S. Kobayashi: *Eng. Fail. Anal.*, **15** (2008), 261.
13) N.-A. Noda, Hendra, M. Oosato, K. Suzumoto, Y. Takase and W. Li: *Key Eng. Mater.*, **462** (2011), 1140.
14) S. Matsuda, D. Suryadi, N.-A. Noda, Y. Sano, Y. Takase and S. Harada: *Trans. Jpn. Soc. Mech. Eng. A*, **79** (2013), 989 (in Japanese).
15) N.-A. Noda, D. Suryadi, S. Matsuda, Y. Sano and Y. Takase: *ISIJ Int.*, **55** (2015), 2416.
16) S. Harada, N.-A. Noda, O. Uehara and M. Nagano: *Trans. Jpn. Soc. Mech. Eng. A*, **57** (1991), 1637 (in Japanese).
17) N.-A. Noda, Y. Sano, Y. Takase, S. Harada, D. Suryadi and S. Kumasaki: *Tetsu-to-Hagané*, **101** (2015), 284 (in Japanese).
18) Marc Mentat team: Theory and User Information, Vol. A, MSC Software, Tokyo, (2012), 713.
19) Marc Mentat team: Theory and User Information, Vol. A, MSC Software, Tokyo, (2012), 545.
20) Marc Mentat team: Theory and User Information, Vol. A, MSC Software, Tokyo, (2012), 572.